

# Nanoscale

Accepted Manuscript



This is an *Accepted Manuscript*, which has been through the Royal Society of Chemistry peer review process and has been accepted for publication.

*Accepted Manuscripts* are published online shortly after acceptance, before technical editing, formatting and proof reading. Using this free service, authors can make their results available to the community, in citable form, before we publish the edited article. We will replace this *Accepted Manuscript* with the edited and formatted *Advance Article* as soon as it is available.

You can find more information about *Accepted Manuscripts* in the [Information for Authors](#).

Please note that technical editing may introduce minor changes to the text and/or graphics, which may alter content. The journal's standard [Terms & Conditions](#) and the [Ethical guidelines](#) still apply. In no event shall the Royal Society of Chemistry be held responsible for any errors or omissions in this *Accepted Manuscript* or any consequences arising from the use of any information it contains.

Cite this: DOI: 10.1039/c0xx00000x

www.rsc.org/xxxxxx

ARTICLE TYPE

# Rapid synthesis of PtRu nano-sponge with different surface compositions and performance evaluation for methanol electrooxidation

Meiling Xiao,<sup>a</sup> Ligang Feng,<sup>b\*</sup> Jianbing Zhu,<sup>a</sup> Changpeng Liu,<sup>c</sup> and Wei Xing<sup>a\*</sup>

Received (in XXX, XXX) Xth XXXXXXXXX 20XX, Accepted Xth XXXXXXXXX 20XX

DOI: 10.1039/b000000x

A rapid strategy to synthesize highly active PtRu alloy nano-sponge catalyst system for methanol electrooxidation was presented. The greatly increased Pt utilization, anti-CO poisoning ability and electronic effect resulting from the porous nano-sponge structure could account for the performance improvement.

## Introduction

Methanol electrooxidation reaction have received considerable attention due to the development of direct methanol fuel cells, which are considered to be one of the promising clean energy sources<sup>1</sup>; meanwhile, methanol as a simple one carbon organic molecules, is worthy of studying as a model for understanding the fundamental theory of electrocatalytic reactions<sup>2</sup>. So far, PtRu is considered as the best catalyst system to obtain both high catalytic activity and stability for methanol electrooxidation resulting from the nice catalytic synergy<sup>3</sup>. Thus, a so-called bifunctional mechanism was proposed to address the role of Ru in the PtRu system, where Ru facilitates generation of hydroxyls to oxidize the poison species and thus releases the occupied active sites<sup>4</sup>. In order to maximize the role of Ru, rational design of PtRu structure is highly desired by means of nanotechnology.

Nanoporous materials with interconnected nanoscale skeletons and voids have been proved to present a particular multifunctional catalytic nano-architecture, show great potential application in electro-catalytic<sup>5</sup>. To date, great efforts have been devoted to the synthesis of nanoporous metals. For example, various Pt-based alloys with nanoporous structure, including PtFe, PtCu, PtCo, PtAu, PtRu were fabricated<sup>6</sup>. Among which nanoporous PtRu shows remarkable superiority for methanol oxidation reaction<sup>7</sup>. The interconnected ligaments in nanoporous PtRu have curved surfaces dominated by highly active low-coordinated atoms, such as steps and kinks, which serve as excellent catalytic sites for methanol oxidation reaction<sup>8</sup>. Beside, owing to the extensive porous networks, the diffusivity within nanoporous PtRu is greatly enhanced, which facilitates the mass transfer of reactants from exterior surface to the interior structure, significantly enhancing the catalytic reactions<sup>5d, 95d, 95d, 915, 24, 2516, 25, 2615, 24, 2516, 8-10</sup>. However, the approaches reported previously were carried out under rigorous condition that was often time-consuming, complicated and dangerous<sup>16, 23, 24</sup>.

Therefore, facile synthetic methods suitable for large-scale production are highly desired. In the present work, we report a

rapid strategy to synthesize highly active PtRu alloy nano-sponge catalyst system for methanol electrooxidation. By tuning the ratio of Pt/Ru in the feeding solution, composition-adjustable PtRu alloys can be obtained easily. The catalysts samples were thoroughly characterized by physical and electrochemical technologies. The greatly increased Pt utilization, anti-CO poisoning ability and electronic effect resulting from the nanoporous sponge structure significantly increased the methanol electrooxidation ability.

## Experimental details

PtRu nano-sponge was fabricated by reducing Pt and Ru precursors with NaBH<sub>4</sub> aqueous solution. Take Pt<sub>1</sub>Ru<sub>1</sub> nano-sponge as an example, aqueous solution (10 mL) of 0.05 M H<sub>2</sub>PtCl<sub>6</sub> and 0.05 M RuCl<sub>3</sub> was quickly injected into 50 mL of NaBH<sub>4</sub> aqueous solution (0.1 M) under vigorous stirring. The stirring was continued for about 5 min until the entire solution became colorless. Then, the mixture was centrifuged and washed with Millipore-MiliQ water, and dried at room temperature finally. In a similar method, Pt<sub>3</sub>Ru<sub>1</sub>, Pt<sub>1</sub>Ru<sub>3</sub> and Pt<sub>1</sub>Ru<sub>4</sub> nano-sponges were fabricated by varying the atomic ratios of Pt/Ru in the feeding solution.

Transmission electron microscopy (TEM), high resolution transmission electron microscopy (HRTEM), high-annular dark-field scanning transmission electron microscopy (STEM) and element mapping analysis were conducted on Philips TECNAI G2 electron microscope operating at 200 kV. Scanning electron microscopy (SEM) measurements and energy-dispersive X-ray (EDX) spectroscopy were performed on an XL 30 ESEM FEG field emission scanning electron microscope. The bulk compositions of the PtRu nano-sponges were evaluated by inductively coupled plasma optical emission spectrometer (X Series 2, Thermo Scientific USA). X-ray diffraction (XRD) measurements were performed with a PW-1700 diffractometer using a Cu K<sub>α</sub> (λ=1.5405 Å) radiation source (Philips Co.). X-ray photoelectron spectroscopy (XPS) measurements were carried out on Mg K<sub>α</sub> radiation source (Kratos XSAM-800 spectrometer).

Electrochemical measurements were carried out with an EG&G mode 273 potentiostat/galvanostat and a conventional three-electrode test cell. A Pt foil and a saturated calomel electrode (SCE) were used as the counter and the reference electrodes, respectively. All of the potentials are related to SCE electrode, unless otherwise noted. The working electrode was

prepared in the same way as in our previous work<sup>11</sup>. Cyclic voltammetry experiments were carried out in 0.5 M H<sub>2</sub>SO<sub>4</sub> + 1 M CH<sub>3</sub>OH solution saturated with N<sub>2</sub> at a scan rate of 50 mV s<sup>-1</sup>. Chronoamperometric experiments were performed in 0.5 M H<sub>2</sub>SO<sub>4</sub> + 1 M CH<sub>3</sub>OH solution at 0.5 V. The electrochemical impedance spectra were recorded at the frequency range from 100 kHz to 10 mHz with 10 points per decade. The amplitude of the sinusoidal potential signal was 5 mV. For CO stripping experiment, CO was absorbed at 0.02 V for 10 min in 0.5 M H<sub>2</sub>SO<sub>4</sub> solution, excess CO in the electrolyte was then purged out with N<sub>2</sub> for 10 min, and then first two cycles were recorded at 20 mV s<sup>-1</sup>. The electrochemical active specific surface area was evaluated by integration of the CO<sub>ad</sub> stripping peak and the coulombic charge required for a monolayer of CO oxidation is 420 μC cm<sup>-2</sup>.

## Results and discussion

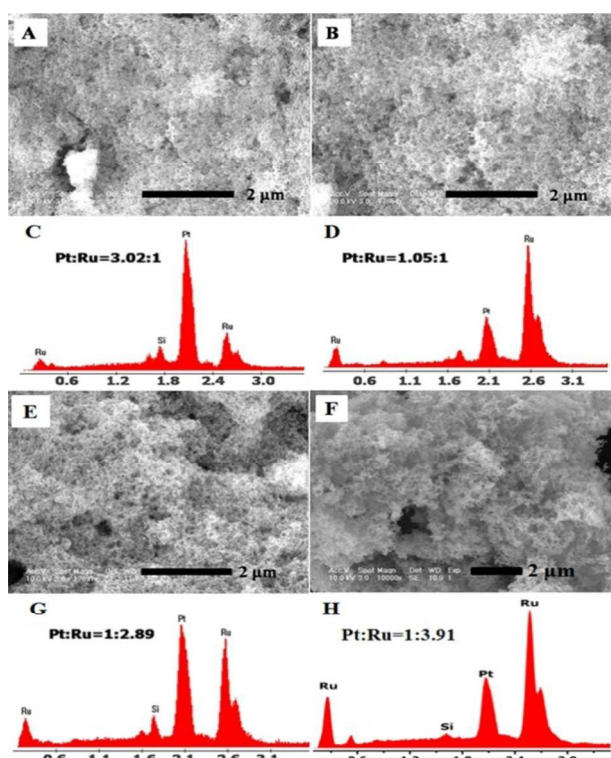


**Fig.1** SEM images and the corresponding EDX patterns of Pt<sub>3</sub>Ru<sub>1</sub> (A, C), Pt<sub>1</sub>Ru<sub>1</sub> (B, D), Pt<sub>1</sub>Ru<sub>3</sub> (E, G) and Pt<sub>1</sub>Ru<sub>4</sub> (F, H).

The morphology of the prepared PtRu nano-sponge was characterized by SEM and TEM technologies. Representative SEM images of PtRu nano-sponges are shown in Fig. 1. Interconnected networks are observed on all the samples, but the surface becomes much looser and more porous by increasing Ru/Pt ratio. The atomic ratio of Pt/Ru obtained from EDX results agreed well with the nominal Pt/Ru ratio in the feeding solution. Typical TEM images are shown in Fig. 2A-D. Observation of the nanoporous networks indicates that the ligaments are not of uniform size and often featured with many branches of similar size. HRTEM image of Pt<sub>1</sub>Ru<sub>3</sub> nano-sponge is also shown here as an example (Fig. 2E), the single-crystalline structure with highly ordered continuous fringe patterns is observed with the interplanar spacing of 0.22 nm, which corresponds to the (111)

crystal plane of PtRu alloy structure. The element mapping was done on a randomly selected area, and a typical result illustrates the uniform distribution of both Pt and Ru elements (Fig. 2F-H), revealing the formation of the alloy structure after simultaneous reduction by strong reducing agent of NaBH<sub>4</sub>.

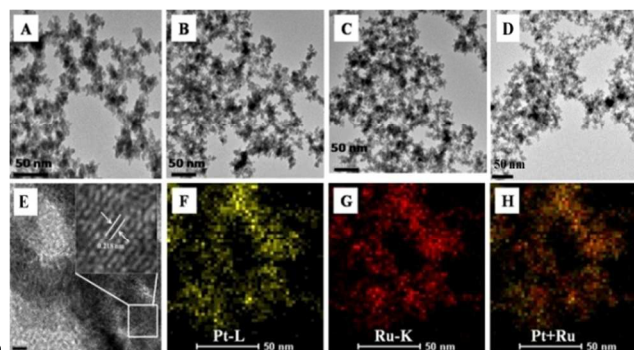


**Fig.2** (A-D) TEM images of Pt<sub>3</sub>Ru<sub>1</sub>, Pt<sub>1</sub>Ru<sub>1</sub>, Pt<sub>1</sub>Ru<sub>3</sub>, and Pt<sub>1</sub>Ru<sub>4</sub> (E) HRTEM images of the Pt<sub>1</sub>Ru<sub>3</sub> nano-sponge and (F-H) STEM image with the corresponding elemental mapping images.

XRD was used to analyze the crystalline structure of PtRu samples. It is noted that the diffraction patterns for all samples are quite similar to each other with a strong peak at around 41.0°, which can be assigned to the (111) reflection; while reflections corresponding to (200) and (220) planes are very weak (Fig. 3A). Similar patterns were also reported on nanoporous PtRu alloy<sup>7</sup>. By increasing Ru content, the diffraction peaks shifted to the higher angle, indicating a lattice contraction due to the substitution of smaller Ru atoms. The broader peak of (111) reflection on Pt<sub>1</sub>Ru<sub>3</sub> is a sign of more Ru atoms distributed on the cubic lattice sites of Pt. The higher (111) reflection intensity reveals that the PtRu nanocrystals have preferentially oriented crystalline structure with (111) planes to the supporting substrate, which is in good agreement with HRTEM observations. Fig. 3B shows the XPS spectra for Pt 4f and Ru 3p core level region for all samples. The atomic ratio of Pt/Ru on the surface of Pt<sub>3</sub>Ru<sub>1</sub>, Pt<sub>1</sub>Ru<sub>1</sub>, Pt<sub>1</sub>Ru<sub>3</sub> and Pt<sub>1</sub>Ru<sub>4</sub> was calculated to be 2.16/1, 1/1.52, 1/3.24 and 1/4.19, respectively. Apparently, the atomic ratio of Pt/Ru on surface is lower than that in the bulk for all PtRu samples. This should result from the different reduction potentials of Pt and Ru, in which it is more difficult for the reduction of Ru. Compared with monometallic Pt, a positive shift of Pt 4f peak suggests a lowering of the Fermi level or an increase of the d-vacancy, resulting in an enhanced CO tolerance on PtRu alloys<sup>12</sup>. With the increase of Ru content, the peak position positive shifts to higher binding energy (BE) for both Pt and Ru elements. All these results indicated that the incorporation of Ru into Pt can effectively modified the electronic structure of Pt atoms and stronger electronic interaction of Pt and Ru was achieved on the Ru-enrich Pt<sub>1</sub>Ru<sub>3</sub> sample. Therefore, improved catalytic activity of Pt toward methanol oxidation is expected on Pt<sub>1</sub>Ru<sub>3</sub> sample.

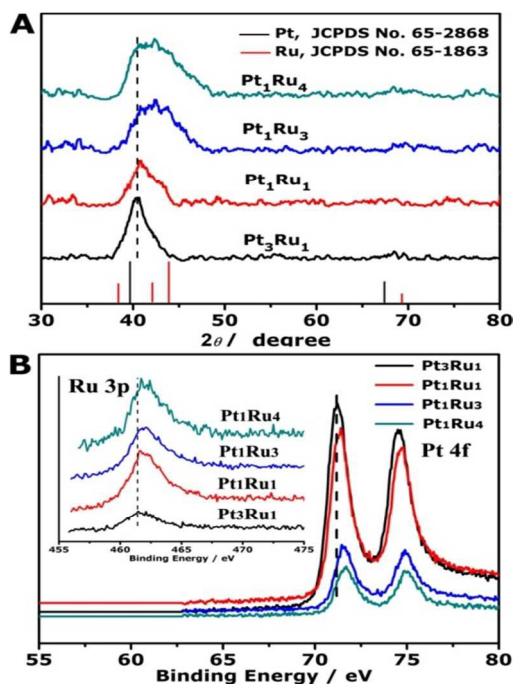


**Fig.3** (A) XRD patterns of PtRu nano-sponges, (B) XPS spectra of Pt 4f and Ru 3p (inset) for PtRu nano-sponges. The dashed line represents location of Pt 4f line for pure Pt.

Fig. 4A displays the cyclic voltammograms (CVs) of the as-prepared PtRu catalysts and commercial PtRu black in 0.5 M  $\text{H}_2\text{SO}_4$ +1 M  $\text{CH}_3\text{OH}$  solution saturated by  $\text{N}_2$ . The activity of PtRu electrocatalysts for methanol oxidation can be represented by the magnitude of the forward anodic current peak. All the nanoporous PtRu catalysts demonstrated much higher peak current density than that of the commercial PtRu black. Specifically,  $\text{Pt}_1\text{Ru}_3$  possessed the highest activity with a peak current density of  $410 \text{ mA mg}^{-1}_{\text{Pt}}$ , which is about 2.8 times that of the commercial PtRu black ( $148 \text{ mA mg}^{-1}_{\text{Pt}}$ ) and higher than a commercial Pt/C catalyst reported previously (about  $160 \text{ mA mg}^{-1}_{\text{Pt}}$  at 0.5 V)<sup>13</sup>. This optimal composition is different from PtRu nanoparticles; there are some controversies about the composition, though generally an atomic ratio of 1:1 was reported as the optimal composition<sup>14</sup>. It might be due to the different kinds of nano-structure, in which  $\text{Pt}_1\text{Ru}_3$  has a much looser surface than  $\text{Pt}_1\text{Ru}_1$ , thus more accessible active sites could be achieved on the  $\text{Pt}_1\text{Ru}_3$ . Chronoamperometric experiments were also conducted to evaluate the catalytic stability as shown in Fig. 4B. The current decay mainly resulted from the inhibition of surface reaction active sites by accumulated  $\text{CO}_{\text{ad}}$  poisoning species on the catalyst surface. It can be found that  $\text{Pt}_1\text{Ru}_3$  shows the highest steady-state current throughout the whole period. All nanoporous PtRu catalysts demonstrated much higher catalytic activity than that of the commercial PtRu black indicating the advantages of the nano-sponge structure.

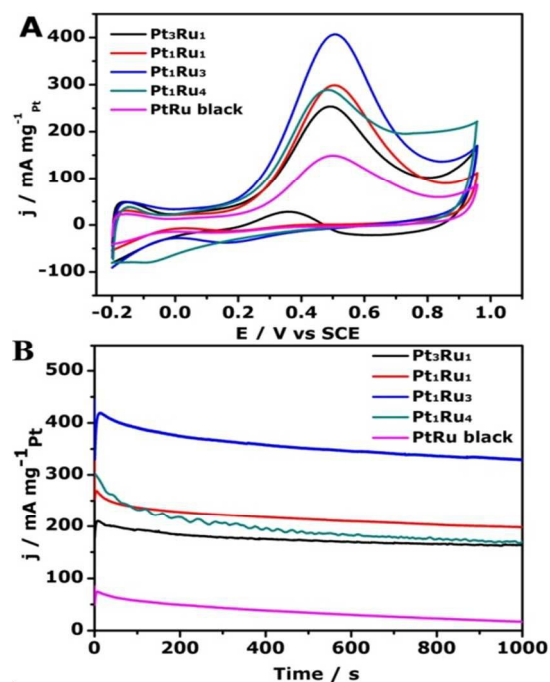


**Fig.4** (A) CVs of PtRu catalysts in 0.5 M  $\text{H}_2\text{SO}_4$ +1 M  $\text{CH}_3\text{OH}$  solution at a scan rate of  $50 \text{ mV s}^{-1}$ , (B) CA curves of PtRu catalysts in 0.5 M  $\text{H}_2\text{SO}_4$ +1 M  $\text{CH}_3\text{OH}$  solution at 0.5 V vs SCE.

Fig. 5A shows the Nyquist plots for the impedance data collected at 0.4 V for all the samples. The diameter of the semicircle or arc correlates with charge transfer resistance. The smaller the diameter indicates the lower the resistance and thus the higher the methanol oxidation rate. It is evident that  $\text{Pt}_1\text{Ru}_3$  has the smallest diameter, thus the highest methanol oxidation activity was observed.

CO stripping experiments were carried out to investigate the anti-poisoning ability as well as estimate the electrochemical active surface area (ECSA), and they are shown in Fig. 5B. The peak potential for CO oxidation on the commercial PtRu catalysts is centered at 0.36 V, while the peak potential is negatively shifted on the PtRu nano-sponge samples. Increasing Ru content will drastically shift the peak value from 0.292 V to 0.251 V, indicating the increased ability for CO oxidation. According to above results, one of the reasons for the enhanced catalytic properties of nanoporous PtRu catalysts toward methanol oxidation is due to the improved CO tolerance. This trend is different from the previous work<sup>23</sup> where they observed ‘increasing the Ru content will shift the CO-stripping peak to more positive potential’ and a similar CO-stripping peak position to the commercial PtRu catalyst. The differences may come from the different PtRu catalysts preparation methods. Based on our results, the catalysts prepared in this work have higher CO tolerance and even more catalytic activity. The ECSA was calculated to be 28.9, 40.9, 48.4, 25.7 and  $35.8 \text{ m}^2 \text{ g}^{-1}$  for  $\text{Pt}_3\text{Ru}_1$ ,  $\text{Pt}_1\text{Ru}_1$ ,  $\text{Pt}_1\text{Ru}_3$ ,  $\text{Pt}_1\text{Ru}_4$  and PtRu black, respectively. Since ECSA can reflect the utilization of Pt, a higher ECSA of the nanoporous PtRu catalysts could also account for the enhanced electrocatalytic activity.

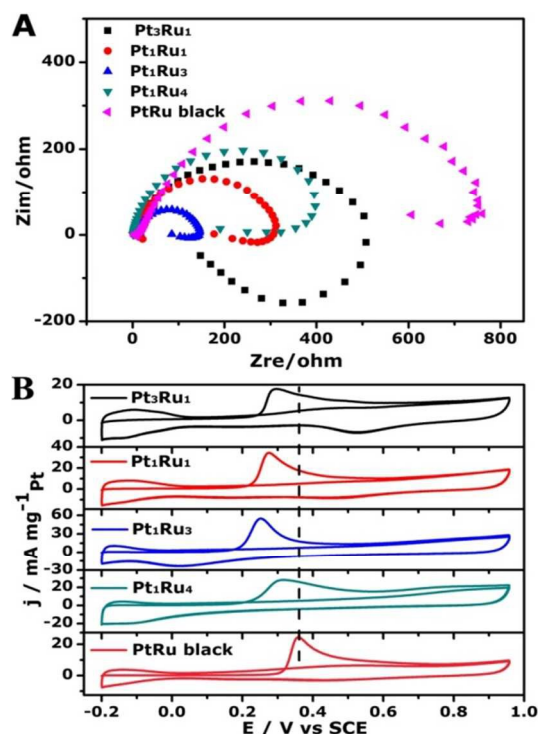


**Fig.5** (A) Nyquist plots of PtRu catalysts for methanol oxidation at 0.4V and (B) CO stripping voltammograms of PtRu catalysts at a scan rate of 20 mV s<sup>-1</sup>.

Based on the experiments above, it can be concluded that the as-prepared PtRu nano-sponge catalysts possess good catalytic performances for methanol oxidation. Specifically, Pt<sub>1</sub>Ru<sub>3</sub> catalyst exhibited the highest catalytic activity. By increasing the Ru contents, surface electronic structure of Pt was modified due to the incorporation of Ru into Pt; thus, higher catalytic activity for methanol oxidation was observed. This is different from PtRu nanoparticle, in which Pt<sub>1</sub>Ru<sub>1</sub> is the optimal composition for methanol oxidation. That may result from the porous nano-sponge structure, in which the presence of Ru largely increases the Pt utilization. According to the bifunctional mechanism, the presence of Ru will facilitate the generation of hydroxyls to oxidize the poison species, thus higher anti-CO poisoning ability and methanol oxidation activity and stability were observed on Pt<sub>1</sub>Ru<sub>3</sub> nano-sponge catalyst system.

## Conclusions

We demonstrate a facile wet-chemical route to prepare highly active PtRu nano-sponge catalyst system for methanol oxidation. By increasing the Ru contents, the surface electronic structure of Pt was improved due to the incorporation of Ru into Pt; thus, higher catalytic activity for methanol oxidation was found on Ru-enriched Pt<sub>1</sub>Ru<sub>3</sub> catalyst. The high performances may result from the porous nano-sponge structure, in which the presence of Ru largely increases the Pt utilization; thus higher anti-CO poisoning ability and methanol oxidation activity and stability were observed on the Pt<sub>1</sub>Ru<sub>3</sub> nano-sponge catalyst system.

## Acknowledgements

The work is financially supported by the National Natural

Science Foundation of China (21373199), the National Basic Research Program of China (973 Program, 2012CB215500, 2012CB932800), and the Strategic priority research program of CAS (XDA0903104).

## Notes and references

<sup>a</sup> State Key Laboratory of Electroanalytical Chemistry, Changchun Institute of Applied Chemistry, Chinese Academy of Sciences, 5625

Renmin Street, Changchun 130022, PR China. E-mail:

xingwei@ciac.ac.cn

<sup>b</sup> Department of Applied Physics, Chalmers University of Technology, SE-41 296, Göteborg, Sweden. E-mail: ligang.feng@chalmers.se;

fenglg11@gmail.com

<sup>c</sup> Laboratory of Advanced Power Sources, Changchun Institute of Applied Chemistry, 5625 Renmin Street, Changchun 130022, PR China.

† Electronic Supplementary Information (ESI) available: [details of any supplementary information available should be included here]. See DOI: 10.1039/b000000x/

‡ Footnotes should appear here. These might include comments relevant to but not central to the matter under discussion, limited experimental and spectral data, and crystallographic data.

1 (a) L. Feng, W. Cai, C. Li, J. Zhang, C. Liu and W. Xing, *Fuel*, 2012, **94**, 401-408; (b) M. B. Zhang, T. Yan and J. G. Gu, *J. Power Sources*, 2014, **247**, 1005-1010; (c) X. Zhao, M. Yin, L. Ma, L. Liang, C. Liu, J. Liao, T. Lu and W. Xing, *Energy Environ. Sci.*, 2011, **4**, 2736-2753.

2 (a) S. Bong, Y. R. Kim, I. Kim, S. Woo, S. Uhm, J. Lee and H. Kim, *Electrochemistry Communications*, 2010, **12**, 129-131; (b) T. Huang, J. L. Liu, R. S. Li, W. B. Cai and A. S. Yu, *Electrochemistry Communications*, 2009, **11**, 643-646; (c) L. Feng, Q. Lv, X. Sun, S. Yao, C. Liu and W. Xing, *J. Electroanal. Chem.*, 2012, **664**, 14-19; (d) L. Feng, X. Zhao, J. Yang, W. Xing and C. Liu, *Catal. Commun.*, 2011, **14**, 10-14.

3 (a) Y. S. Kim, S. H. Nam, H. S. Shim, H. J. Ahn, M. Anand and W. B. Kim, *Electrochemistry Communications*, 2008, **10**, 1016-1019; (b) Z. Q. Jiang and Z. J. Jiang, *Electrochim Acta*, 2011, **56**, 8662-8673; (c) K. Koczur, Q. F. Yi and A. C. Chen, *Adv Mater*, 2007, **19**, 2648-+; (d) C. Nethravathi, E. A. Anumol, M. Rajamathi and N. Ravishankar, *Nanoscale*, 2011, **3**, 569-571.

4 (a) K. W. Park and Y. E. Sung, *J Phys Chem B*, 2005, **109**, 13585-13589; (b) M. Watanabe and S. Motoo, *J Electroanal Chem*, 1975, **60**, 267-273.

5 (a) S. J. Guo, S. J. Dong and E. K. Wang, *Chem Commun*, 2010, **46**, 1869-1871; (b) C. Y. Du, M. Chen, W. G. Wang and G. P. Yin, *Acs Appl Mater Inter*, 2011, **3**, 105-109; (c) J. Liu, L. Cao, W. Huang and Z. L. Li, *Acs Appl Mater Inter*, 2011, **3**, 3552-3558; (d) C. X. Xu, Y. Q. Liu, J. P. Wang, H. R. Geng and H. J. Qiu, *Acs Appl Mater Inter*, 2011, **3**, 4626-4632; (e) L. L. Wang, D. F. Zhang and L. Guo, *Nanoscale*, 2014, **6**, 4635-4641; (f) Y. L. Wang, Y. C. Zhu, J. J. Chen and Y. Zeng, *Nanoscale*, 2012, **4**, 6025-6031; (g) J. Ying, X. Y. Yang, G. Tian, C. Janiak and B. L. Su, *Nanoscale*, 2014, **6**, 13370-13382.

6 (a) C. X. Xu, R. Y. Wang, M. W. Chen, Y. Zhang and Y. Ding, *Phys Chem Chem Phys*, 2010, **12**, 239-246; (b) Z. H. Zhang, Y. Wang, Z. Qi, W. H. Zhang, J. Y. Qin and J. Frenzel, *J Phys Chem C*, 2009, **113**, 12629-12636; (c) D. S. Wang, P. Zhao and Y. D. Li, *Sci Rep-Uk*, 2011, **1**.

7 C. X. Xu, L. Wang, X. L. Mu and Y. Ding, *Langmuir*, 2010, **26**, 7437-7443.

8 T. Fujita, P. F. Guan, K. McKenna, X. Y. Lang, A. Hirata, L. Zhang, T. Tokunaga, S. Arai, Y. Yamamoto, N. Tanaka, Y. Ishikawa, N. Asao, Y. Yamamoto, J. Erlebacher and M. W. Chen, *Nat Mater*, 2012, **11**, 775-780.

9 (a) S. J. Guo, S. J. Dong and E. K. Wang, *J Phys Chem C*, 2010, **114**, 4797-4802; (b) P. A. Ganesh and D. Jeyakumar, *Nanoscale*, 2014, **6**, 13012-13021.

10 H. Hoster, T. Iwasita, H. Baumgartner and W. Vielstich, *J Electrochem Soc*, 2001, **148**, A496-A501.

11 J. Chang, L. Feng, C. Liu, W. Xing and X. Hu, *Energy Environ. Sci.*,

- 
- 2014, **7**, 1628-1632.
- 12 H. Igarashi, T. Fujino, Y. M. Zhu, H. Uchida and M. Watanabe, *Phys Chem Chem Phys*, 2001, **3**, 306-314.
- 13 (a) M. L. Xiao, S. T. Li, X. Zhao, J. B. Zhu, M. Yin, C. P. Liu and W. Xing, *Chemcatchem*, 2014, **6**, 2825-2831; (b) J. B. Zhu, M. L. Xiao, X. Zhao, K. Li, C. P. Liu and W. Xing, *Chem Commun*, 2014, **50**, 12201-12203.
- 14 (a) L. Zou, J. Guo, J. Liu, Z. Zou, D. L. Akins and H. Yang, *J. Power Sources*, 2014, **248**, 356-362; (b) Z. G. Shao, F. Y. Zhu, W. F. Lin, P. A. Christensen and H. M. Zhang, *Phys Chem Chem Phys*, 2006, **8**, 2720-2726; (c) C. Bock, B. MacDougall and Y. LePage, *J. Electrochem. Soc.*, 2004, **151**, A1269-A1278.